Growth and structural properties of epitaxial $Ga_xIn_{1-x}P$ on InP

A. Bensaada, A. Chennouf, R. W. Cochrane, and R. Leonelli
Groupe de recherche en physique et technologie des couches minces and Département de physique, Université de Montréal, C.P. 6128 Succ. A., Montréal, Québec H3C 3J7, Canada

P. Cova and R. A. Masut
Groupe de recherche en physique et technologie des couches minces and Département de génie physique, Ecole Polytechnique, C.P. 6079 Succ. A, Montréal, Québec H3C 3A7, Canada

(Received 31 July 1991; accepted for publication 13 November 1991)

The growth of heteroepitaxial $Ga_xIn_{1-x}P$ on InP for $0<x<0.25$ has been carried out by low-pressure metalorganic chemical vapor deposition and characterized by high-resolution x-ray diffraction and low-temperature photoluminescence measurements. The x-ray data indicate that the epilayers are under biaxial tensile strain and that, for samples with $x<0.05$, the lattice mismatch is accommodated almost completely by tetragonal distortions. From photoluminescence measurements, the energy band gap is found to vary monotonically with the Ga concentration; it also shifts linearly with the elastic strain in the layer. The calculated value of 0.99×10^4 meV per unit strain is in good agreement with that predicted from elasticity theory.

I. INTRODUCTION

Among the III-V alloy semiconductors, $Ga_xIn_{1-x}P$ has been extensively studied because of its important technological role in the fabrication of high-efficiency light-emitting diodes[1] and visible double heterostructure lasers.[2] $Ga_{0.5}In_{0.5}P$ lattice matched to GaAs is a more efficient red-light-emitting material than other GaAs ternary-related compounds used for this purpose.[3] It can also be used as a wide-gap emitter in a heterostructure bipolar transistor.[4]

Conventionally, for the minimizing of the lattice mismatch, substrate choices for $Ga_xIn_{1-x}P$ depend on x. For $0.85<x<1$, $x\sim0.7$, and $x\sim0.5$, the substrates are, respectively, GaP,[5,6] $GaAs_{0.6}P_{0.4}$,[5] and GaAs.[5,7] However, very little work has been reported on the growth of $Ga_xIn_{1-x}P$ on InP substrates, essentially due to the growth difficulties arising from the lattice mismatch. Recently, another field of application of GaInP has been found: it has been successfully used as a wide-band-gap semiconductor to improve the electrical quality of Schottky diodes on InP.[8,9] Indeed, the introduction of a thin GaInP film (below the critical thickness) between the metal and InP increases significantly the barrier height of the Schottky diodes. The effect of the lattice mismatch between the epitaxial layers and the substrates on the structural, optical, and electrical properties of GaInP has been discussed by several authors. For example, it has been shown that the growth of GaInP epitaxial layers with large lattice mismatch on GaP substrates exhibits a columnar morphology.[10] The harmful effect of the lattice mismatch on the photoluminescence of GaInP epilayers on GaAs has been thoroughly established;[7,11] lattice mismatch has also been found responsible for the deviation from the ideal thermionic behavior of the GaInP-on-InP Schottky diodes.[12]

In this paper, we report the metal-organic chemical vapor deposition (MOCVD) growth and characterization of $Ga_xIn_{1-x}P(0<x<0.25)$ on InP substrates. The effects of the increase of the Ga content on the surface morphology, on the deformation of the epilayer crystal lattice, and on the photoluminescence spectra are also reported.

II. EXPERIMENTAL PROCEDURES

A. MOCVD film growth

The MOCVD growth was carried out using a cold-wall horizontal reactor operating at low pressure using Pd-purified hydrogen as a carrier gas. This system has been described in detail elsewhere.[13] Substrates were mounted on a graphite susceptor and placed in the reactor which consists of a horizontal quartz tube with a rectangular cross section and infrared heater lamps. The growth precursors were trimethylindium (TMIn), trimethylgallium (TMGa), and phosphine (PH_3). TMIn and TMGa bubblers were held at 25 and -12 °C, respectively. Because of the relatively high vapor pressure of TMGa compared to TMIn, a dilution line has been installed to control precisely the TMGa flow. In these experiments the reactor pressure was maintained at 40 Torr, the growth temperature at 640 °C, and the V/III ratio at 200. The typical flow rates used for sample growth were 1.2×10^{-8}–1×10^{-6} mol/min for TMGa, 1.1×10^{-5} mol/min for TMIn, and 2.2×10^{-3} mol/min for PH_3. These growth conditions were slightly different than those that optimize the growth of homoepitaxial InP.[13] The only exception was for the most dilute Ga layer ($x\approx0.02$) where it was necessary to increase the flow rates of both TMIn and PH_3 to 1.65×10^{-5} and 3.35×10^{-3} mol/min, respectively. This change had the effect of doubling the growth rate, an effect which is reflected in several of the measured properties, as explained below.

The substrates used for the heteroepitaxial growth were InP liquid-encapsulated Czochralski (LEC)-grown crystals [(100), S doped, $n\sim10^{18}$ cm^{-3}]. They were first degreased with CMOS grade standard organic solvents: trichlorethane, acetone, and propanol. After being abundantly rinsed in de-ionized water (18 MΩ cm), they were

 0021-8979/92/041737-07$04.00

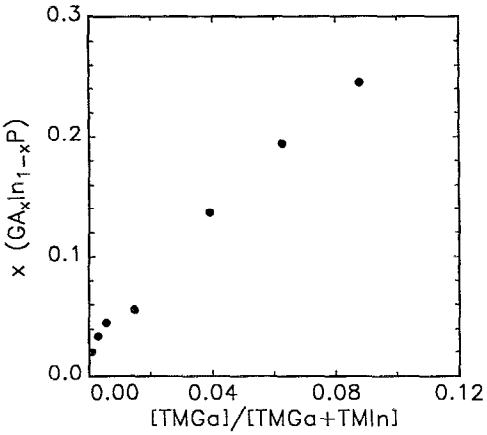

FIG. 1. Solid Ga concentration, x, of the $Ga_xIn_{1-x}P$ epilayers vs the vapor composition [TMGa]/[TmGa + TMIn] for films grown at 640 °C with a V/III ratio of 200.

etched in $H_2SO_4 : H_2O_2 : H_2SO_4$ (4:1:1) for 2 min, rinsed again with de-ionized water, blown dry with N_2, and loaded into the reactor. A pregrowth annealing at 640 °C under PH_3 (introduced when the substrate temperature reached 100 °C) was performed for 10 min to remove the native oxide from the substrate surface, and a 1000-Å buffer layer on InP was grown to improve the interface quality. Thicknesses of the epitaxial layers were in the range 1–1.5 μm.

B. Sample characterization

The surface morphology was examined with a Nomarski interference phase contrast microscope. The epilayer thicknesses were measured using scanning electron micrography (SEM) after the samples had been cleaved and stain-etched in 16 g $K_3Fe(CN)_6$ + 24 g KOH + 140 ml, H_2O solution for 5 s under strong illumination. X-ray diffraction measurements were obtained on a Philips high-resolution five-crystal diffractometer[14] using Cu$K\alpha_1$ radiation with the monochromator aligned in its Ge (220) setting. The mole fraction (x) of Ga in $Ga_xIn_{1-x}P$ and the degree of relaxation were determined by measuring the separation between the peak of the epitaxial layer and that of the substrate in the x-ray rocking curves for symmetrical as well as asymmetrical reflections.[14–16] Finally, the photoluminescence (PL) was excited using the 514.5-nm line of an Ar^+ laser. The signal was dispersed by a 1-m double spectrometer and detected by a cooled InGaAs photomultiplier tube using conventional photon-counting techniques. The sample temperature was maintained at 4.2 K in a liquid-helium cryostat.

III. EXPERIMENTAL RESULTS

A. Growth characteristics

As can be seen from Fig. 1, the amount of gallium incorporated in the solid phase proved a nearly linear function of the TMGa concentration in the vapor phase. Although the surface morphology seems smooth and featureless (Fig. 2), a few dislocation lines appear first in the [01$\bar{1}$] direction in the $x = 0.045$ sample. This behavior is well known and has been repeatedly observed for GaInAs/GaAs.[17] For $x \approx 0.05$, the surface shows a cross-hatched pattern under a microscope (although the surface appears mirrorlike to the naked eye) with dislocations lying in both [011] and [01$\bar{1}$] directions. Above this concentration, the cross-hatch density increases gradually up to the sample richest in Ga ($x = 0.245$) for which the surface is rough. The figure also clearly shows that the dislocation

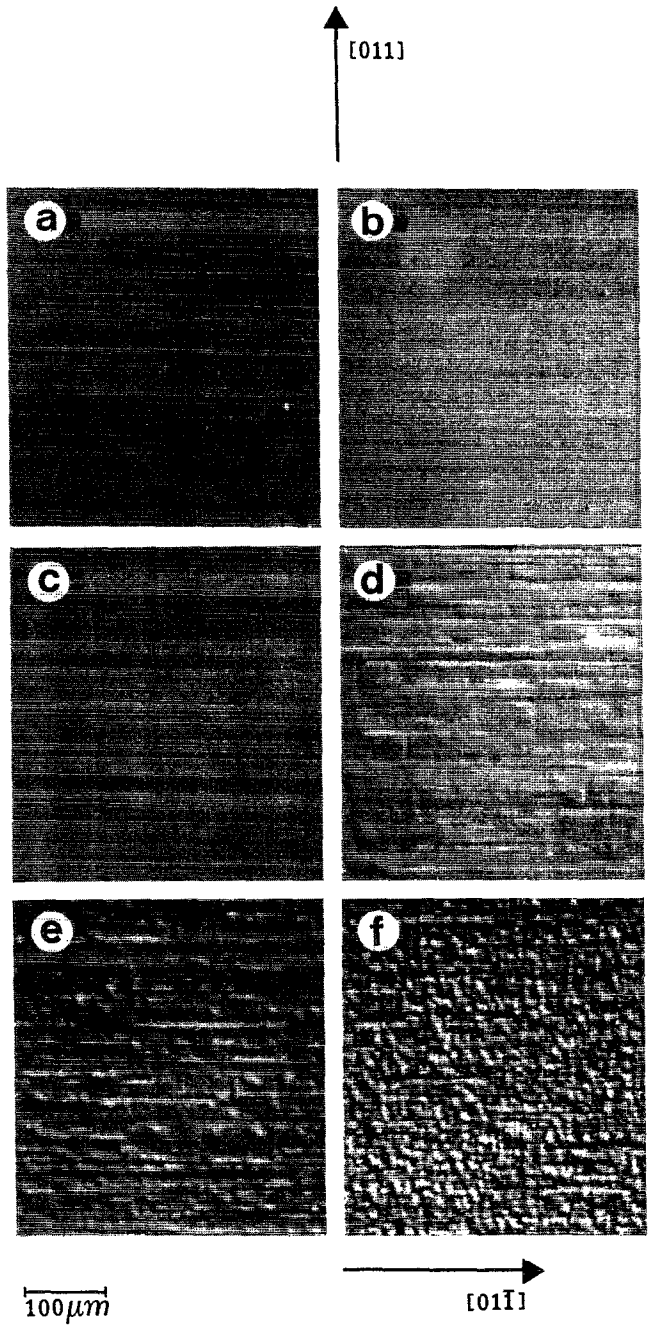

FIG. 2. Surface morphology of $Ga_xIn_{1-x}P$ grown on InP:S (001) by low-pressure MOCVD, with x equal to (a) 0.034, (b) 0.045, (c) 0.055, (d) 0.136, (e) 0.194, and (f) 0.245.

density increases with the gallium composition, i.e., with the lattice mismatch.

Transmission electron microscopy studies indicate that misfit dislocations which cause relaxation at (100) interfaces in zinc-blende structures are predominantly of the 60° type.[18] These dislocations glide in the [111] slip planes to form long segments lying along the [011] directions. Besides causing enhanced impurity diffusion, these segments also cause degradation of optical and electrical properties of the epilayers.[19] It is well known[20] that there exists an elastic limit below which the lattice mismatch is mainly accommodated by elastic deformation. For our samples of thickness 1–1.5 μm and values of x above $\simeq 0.05$, it is energetically favorable to relieve the mismatch by generation of misfit dislocations.

B. X-ray diffraction

The symmetrical (004) x-ray reflection has been used to calculate the epitaxial layer lattice parameter perpendicular to the (100) plane, the full width at half maximum (FWHM) of the epilayer peak being a measure of its crystalline quality. Symmetrical (004) rocking curves were taken for a number of azimuthal angles (rotation around [001] direction) to search for any tilt angle between the crystallographic planes of the substrate and epilayer.[21,22] However, no measurable tilt was observed. Because the epilayers are not fully relaxed, asymmetric (115) and (224) diffraction curves were used to determine the state of strain in the $Ga_xIn_{1-x}P$ layers. From these asymmetric curves were calculated the lattice parameters perpendicular to ($a_\perp$) and parallel to ($a_\parallel$) the (100) surface.[23] The values of the lattice parameter perpendicular to the surface obtained from the symmetric and asymmetric reflections provided an internal consistency verification. A difference between $(\Delta a/a)_\perp$ and $(\Delta a/a)_\parallel$ (where Δa is the difference between the epilayer lattice parameter $a_{\rm epi}$ and that of the substrate a_s) is related to the tetragonal deformation of the unit cell.

The x-ray diffraction curve of the symmetric (004) reflection of $Ga_{0.045}In_{0.955}P$ is presented in Fig. 3. The epitaxial layer peak FWHM is only 48 arcsec compared with the 300 arcsec obtained by Chen *et al.*[12] for their $x = 0.032$ sample; concomitantly, the surface morphology of our sample is apparently smoother than that reported by these same authors.[12]

The epitaxial layer compositions are determined from the lattice parameters of the completely relaxed layers. For the completely relaxed epilayer $(\Delta a/a)_{\rm rel}$ can be calculated from the values of $(\Delta a/a)_\perp$ and $(\Delta a/a)_\parallel$ of the deformed unit cell using elasticity theory. If the epilayer lattice parameter parallel to the (100) surface, $a_\parallel$, is completely constrained to that of the substrate, then[15]

$$\left(\frac{\Delta a}{a}\right)_{\rm rel} = \left(\frac{\Delta a}{a}\right)_\perp \left(\frac{1-\nu}{1+\nu}\right), \tag{1}$$

where ν is the Poisson ratio of the film given, in terms of the elastic coefficients, by $c_{12}/(c_{11}+c_{12})$. The elastic coefficients for $Ga_xIn_{1-x}P$ are obtained from a linear interpolation between those of GaP and InP using an estimated ternary composition.[16,24] For the partially relaxed systems, Eq. (1) becomes[14,16]

$$\left(\frac{\Delta a}{a}\right)_{\rm rel} = \left(\frac{\Delta a}{a}\right)_\perp \left(\frac{1-\nu}{1+\nu}\right) + \left(\frac{\Delta a}{a}\right)_\parallel \left(\frac{2\nu}{1+\nu}\right), \tag{2}$$

which reduces to Eq. (1) when $a_\parallel = a_s$. A knowledge of the cubic lattice parameter $a_{\rm rel}$ then gives the composition of the epilayer. Rather than supposing a linear Vegard's law for the lattice parameter of the ternary compound between InP and GaP, we take the experimental values of Onton *et al.*[25] which can be represented for $0 < x < 0.5$ by

$$a_{\rm rel} = 5.8696 - 0.3380\ x - 0.1614\ x^2. \tag{3}$$

Here, we use the values of 5.8696 and 5.4514 Å for the room-temperature lattice constants of the two constituent binary compounds, InP and GaP, respectively. Inversion of Eq. (3) gives the compositions cited throughout this paper. It should be noted that the concentrations determined in this manner depend also on the validity of the elasticity theory analysis.

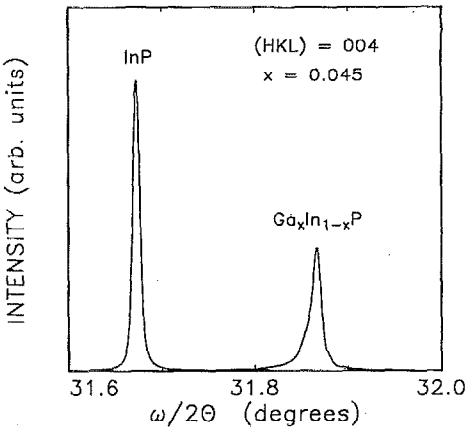

FIG. 3. X-ray diffraction curve of the symmetric (004) reflection of $Ga_{0.045}In_{0.955}P$ on InP:S (100). The GaInP peak FWHM is 48 arcsec.

Based on this simple analysis, the Ga concentration has been determined for each sample. The concentration dependencies of the in-plane and out-of-plane lattice parameters are given in Fig. 4(a); also indicated by the solid line are the bulk values of Eq. (3). Below approximately 5% Ga, the epilayers are accommodated by the biaxial stress. The in-plane lattice parameter $a_\parallel$ is nearly identically that of the InP substrate while $a_\perp$ decreases linearly with x, indicating a tetragonal distortion. Above this value, both parameters approach the bulk value due to the appearance of misfit dislocations but it should be noted that, even for the $x = 0.245$ sample, the relaxation is still not complete.

Figure 4(b) shows the tetragonal deformation of the epilayer as a function of the Ga concentration. For up to 5% Ga the layer is almost completely constrained and the ratio $a_\perp/a_\parallel$ falls linearly with x, as indicated by the dashed line in the figure. This diagram contains the same information as the previous one; in addition, it conveys more

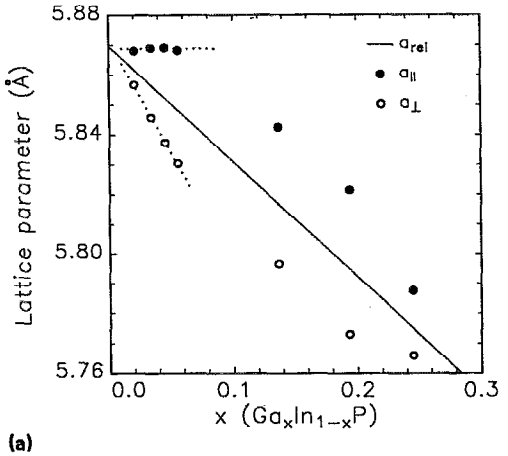

(a)

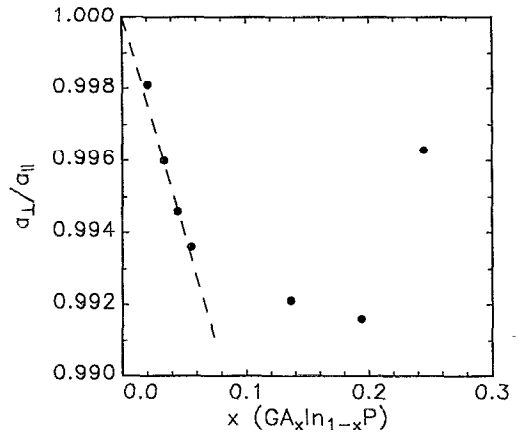

(b)

FIG. 4. (a) Concentration dependence of the lattice parameters, $a_{\perp}$ and $a_{\parallel}$, of $Ga_xIn_{1-x}P$ on InP for $x<0.25$. The solid line represent the relaxed bulk parameters from Eq. (3). (b) Effect of the epilayer composition on the deformation of the lattice, $a_{\perp}/a_{\parallel}$. The dashed line represents the behavior of completely constrained epilayers.

clearly the change in relaxation which occurs at $x\approx 0.05$ where misfit dislocations are formed and the epilayers relax partially. As the Ga content increases above 5%, the epilayers relax progressively so that the deviation from the extension of the dashed curve increases rapidly. At $x=0.245$ the tetragonal distortion has almost been eliminated and the lattice parameters are only slightly different from those of the bulk alloy, as is also evident from Fig. 4(a).

As discussed earlier, when the elastic limit is exceeded, dislocations will nucleate in the interface region in order to relieve a proportion of the misfit strain. The percentage relaxation, R, is defined as

$$R=\frac{a_{\parallel}-a_{\text{sub}}}{a_{\text{rel}}-a_{\text{sub}}}\times 100. \tag{4}$$

It should be noted that in heteroepitaxial growth, the strains existing in the epilayer are usually caused either by the difference in the thermal expansion coefficients of the epilayer and the substrate or by the mismatch in lattice parameters. For our layers, thermal expansion effects can be neglected because of the very small differences of the

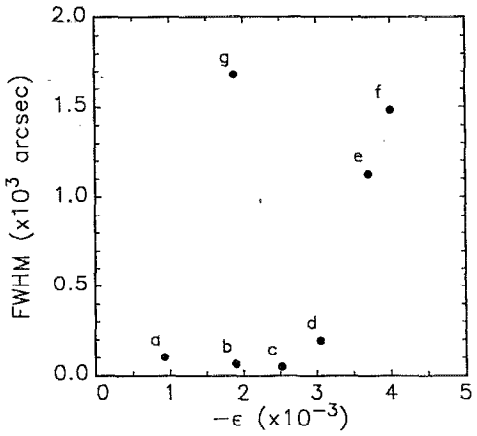

FIG. 5. (004) reflection FWHM of the epilayer x-ray rocking curve peak as a function of the strain for samples with x equal to (a) 0.02, (b) 0.034, (c) 0.045, (d) 0.055, (e) 0.136, (f)0.194, and (g) 0.245.

thermal expansion coefficients of InP and $Ga_xIn_{1-x}P$ for $x<25\%$. Up to a critical thickness the epilayer should, in general, be completely deformed to match their in-plane lattice parameters to that of the substrate, so that the misfit between the two lattices is initially taken up by lattice deformation. As the Ga concentration increases, the critical thickness decreases, and since the epilayer thickness is constant, the lattice deformation should also decrease as there is more relaxation through dislocation generation. This behavior is observed in our GaInP epilayers. The samples with less than 5% Ga have undergone a tetragonal distortion which deforms the in-plane lattice parameter, $a_{\parallel}$, 97% of the way from the bulk value towards that of the substrate. The only exception is the sample with $x=0.02$ for which the epilayer deformation is only 78% toward the substrate, a consequence, we believe, of the faster growth rate of this sample. These results are rather surprising for 1-μm-thick epitaxial layers in view of the fact that the critical thickness for dislocation generation predicted by the simple force-balance model of Matthews and Blakeslee[26] is 0.22 μm for a $Ga_{0.04}In_{0.96}P$ epilayer on InP. For samples with more than 5% Ga, Figs. 4(a) and 4(b) indicate significant relaxation of the epilayers to the point where the $x=0.245$ sample has almost attained the lattice parameters of the bulk alloy.

The x-ray peak linewidths are dominated by the effects of finite epilayer thickness, lattice parameter differences between and within layers, and also by the misorientations between layers. Figure 5 shows the FWHM of the $Ga_xIn_{1-x}P$ peak in the (004) rocking curve as a function of the layer strain, ϵ, defined as

$$\epsilon=\left(\frac{\Delta a}{a}\right)_{\parallel}-\left(\frac{\Delta a}{a}\right)_{\text{rel}}=\left(\frac{1-\nu}{1+\nu}\right)\left[\left(\frac{\Delta a}{a}\right)_{\parallel}-\left(\frac{\Delta a}{a}\right)_{\perp}\right]. \tag{5}$$

The linewidths are small for small ϵ but then increase rapidly with increasing in-plane mismatch. Clearly the epilayer x-ray peaks are broadened when relaxation sets in, mainly because of the mosaicity of the relaxed layers. That

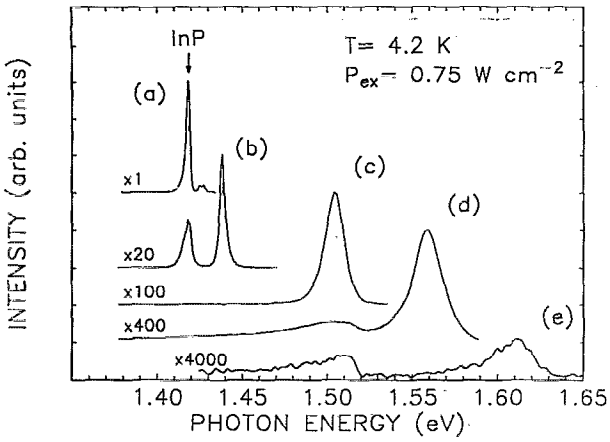

FIG. 6. PL spectra of $Ga_xIn_{1-x}P$ epilayers on InP with x equal to (a) 0.034, (b) 0.055, (c) 0.136, (d) 0.194, and (e) 0.245.

is to say, when dislocations appear, the layer consists of a large number of crystallites tilted slightly with respect to each other. This mosaic spread contributes significantly to the line broadening as dislocations form above 5% Ga but this contribution appears to saturate above about 12% Ga. The linewidth plotted as a function of the layer strain ϵ in Fig. 5 shows a double-valued behavior which is clearly tied to the appearance of the dislocations since they have the effect of lowering the epilayer strain as well as its x-ray quality.

C. Low-temperature photoluminescence

The low-temperature PL spectra of several samples are shown in Figs. 6 and 7. As can be seen, the emission intensities from the GaInP epilayers with less than 5% Ga are all of the same order of magnitude. For the samples with $x = 0.034$ and 0.045, the emission can be resolved into a doublet separated by about 2.2 meV. This value is nearly that of the energy separation between the donor–bound exciton (D^0,X) and carbon acceptor–bound exciton (A^0,X) recombination energy in InP.[27] The doublets are, therefore, attributed to (D^0,X) and (A^0,X) emission in GaInP. The FWHM of each peak in the doublets is less than 2.0 meV, a value which is comparable to that observed in strained InGaAs/GaAs epilayers[28] and which indicates an excellent crystalline quality and homogeneity of these layers. The FWHM of the peak for the $x = 0.055$ sample is about 4.0 meV, indicating an epilayer of good quality and homogeneity. For the $x = 0.02$ sample the linewidth is somewhat larger than those of the best layers, an effect which we attribute to its higher deposition rate.

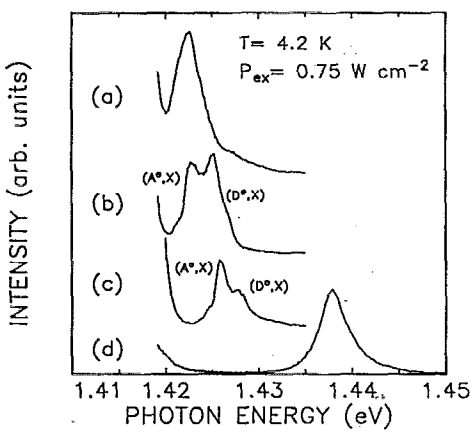

FIG. 7. PL spectra of $Ga_xIn_{1-x}P$ epilayers on InP with x equal to (a) 0.020, (b) 0.034, (c) 0.045, and (d) 0.055.

In addition to the PL from the epilayer, emission from the InP substrate is observed for all the samples with $x < 0.06$. Since the epilayer thicknesses are greater than 1 μm and the penetration depth in InP of light at 514.5 nm is roughly 0.1 μm,[29] this emission cannot originate from direct photoexcitation of the substrate. We rather attribute it to the recombination of photogenerated carriers which have diffused from the epilayer to the substrate. The subsequent emission is detectable because the band gap of the epilayer is larger than that of the substrate and its appearance attests to the high quality of these samples. In the sample with $x = 0.055$, the InP emission decreases by a factor of 40, while in samples with $x > 0.1$, the InP emission is no longer detected and the epilayer emission intensities decrease markedly with an increase of their FWHM. These observations can be correlated with the x-ray peak linewidths (Fig. 5), where a small increase of the FWHM is observed for samples up to $x = 0.055$ and then a much larger one for the $x > 0.1$ samples. It appears then that the multiplication of misfit dislocations, which act as efficient carrier trapping and recombination centers, dramatically reduce the mean free path of the photogenerated carriers and their near-band-gap emission.

The fully relaxed band-gap energies for bulk GaInP at low temperature have been evaluated by Merle *et al.*;[30] in the low x region they find

$$\Delta E_g = E_g(x) - E_g(0) = 0.77\ x + 0.684\ x^2. \qquad (6)$$

In order to determine ΔE_g for our samples, we have assumed that the binding energy of the bound exciton does not vary appreciably throughout the composition range of our samples. ΔE_g can thus be evaluated by subtracting the (D^0,X) and (A^0,X) emission energies in InP (1.416 eV) from either the peak or the mean value of the doublet of the observed GaInP emission bands. In other words, we measure ΔE_g directly from the PL spectra using the relation $\Delta E_g = E_{DA}(x) - E_{DA}(0)$, which we estimate gives the value of ΔE_g to within 1 or 2 meV. These band-gap shifts are presented in Fig. 8 together with the fully relaxed value given by Eq. (6). The almost completely strained epilayers with $x < 0.06$ deviate from the smooth variation of the other films, indicating a strain dependence of the band gap.

Since the GaInP epilayers have a different lattice constant than the substrate, a strain is generated which is expected to induce a uniform shift of the band gap due to a hydrostatic component and to a uniaxial splitting of the $J = \frac{3}{2}$ valence-band edge at $k = 0$.[31] The energy differences between the conduction band and the heavy hole (hh, J

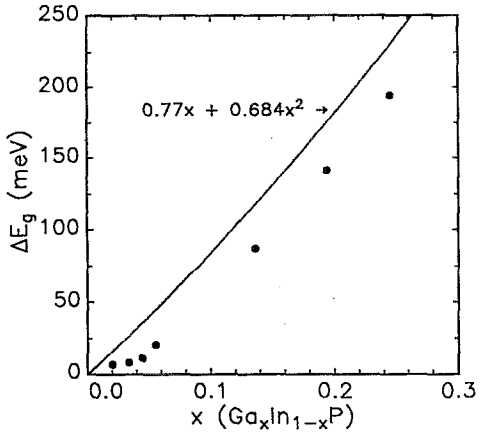

FIG. 8. Band-gap shift of $Ga^xIn_{1-x}P$ as a function of the Ga concentration, x; solid circles: experimental values, solid line: calculated from Eq. (6).

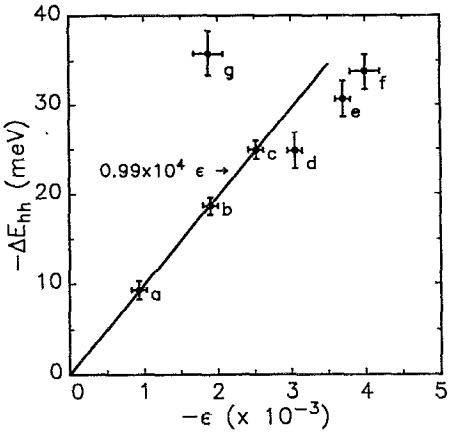

FIG. 9. ΔE_{hh} as a function of strain for samples with x equal to (a) 0.020, (b) 0.034, (c) 0.045, (d) 0.055, (e) 0.136, (f) 0.194, and (g) 0.245. The solid line has been calculated according to Eq. (7a).

$=\frac{3}{2}$, $m=\pm\frac{1}{2}$) or light-hole (lh, $J=\frac{3}{2}$, $m=\pm\frac{3}{2}$) valence bands at $k=0$ should follow[24]

$$\Delta E_{hh}=\left[-2a\left(\frac{c_{11}-c_{12}}{c_{11}}\right)-b\left(\frac{c_{11}+2c_{12}}{c_{11}}\right)\right]\epsilon, \tag{7a}$$

$$\Delta E_{lh}=\left[-2a\left(\frac{c_{11}-c_{12}}{c_{11}}\right)+b\left(\frac{c_{11}+2c_{12}}{c_{11}}\right)\right]\epsilon, \tag{7b}$$

where the hydrostatic deformation potentials for InP at room temperature are $a=-8.0$ eV and $b=-1.55$ eV and the misfit strain ϵ is given by Eq. (5). In the present case, the epilayers are under tension ($\epsilon<0$) and the strain-induced band shift is calculated to be $\Delta E^{hh}=1.03\times10^4\,\epsilon$ (meV). The heavy-hole valence-band shifts were then determined by subtracting the value calculated from Eq. (6) from the experimentally determined values. As can be seen in Fig. 9, ΔE_{hh} varies linearly with strain for the samples with $x<0.05$ with a slope equal to $(0.99\pm0.05)\times10^4$ (meV per unit strain), in excellent agreement with the above estimate. This agreement is surprisingly good since the misfit strain, the stiffness coefficients, and the deformation potential values used in the calculation were those for the samples at room temperature, whereas the PL was performed at 4.2 K. However, it should be noted that a similar agreement between low-temperature PL measurements and room-temperature strain-induced valence-band shifts was also observed in $Ga_xIn_{1-x}P/GaAs$ with $x=0.51$.[32] Only the sample richest in Ga ($x=0.245$) deviates significantly from the linear relation, leading us to conclude that its PL originates from regions which are less relaxed than the average relaxation values determined by the x-ray measurements.[33] A further conclusion from Fig. 9 is that the partially relaxed films from 5% to 17% Ga are quite uniform since the ΔE_{hh} values (derived from the PL measurements) continue to follow the same strain dependence (deduced from the XRD data) as the completely strained samples below 5% Ga.

IV. CONCLUSION

Epitaxial layers of $Ga_xIn_{1-x}P(x<0.25)$ have been grown on InP by low-pressure MOCVD. The lattice mismatch of these relatively thick (1–1.5 μm) epilayers is largely accommodated by lattice deformation up to a limiting value of $x\approx0.05$ corresponding to a misfit strain of $\approx3\times10^{-3}$. (004) x-ray reflection FWHM and low-temperature photoluminescence of these layers indicate that they are of good crystalline quality, although there is evidence that high growth rates result in poorer crystal quality. For $x>0.05$, the generation of a large concentration of dislocations takes place in order to relieve the lattice mismatch; even at $x=0.25$ the 1-μm-thick layers are not fully relaxed. The biaxial stress in these films results in an energy-band-gap shift of 0.99×10^4 per unit strain, a value which is in good agreement with that calculated from elasticity theory.

ACKNOWLEDGMENTS

The authors acknowledge useful discussions with several members of the GCM as well as the technical assistance of R. Lacoursiere. This research has been supported by the NSERC Canada and Fonds FCAR Québec. Two of the authors (A.B. and A.C.) would like to acknowledge financial support of the Department of Physics, University of Oran, Algeria.

[1] R. J. Archer, J. Electron. Mater. **1**, 128 (1972).
[2] I. Hino and T. Suzuki, J. Cryst. Growth **68**, 483 (1984).
[3] T. Iwamoto, K. Mori, M. Mizuta, and H. Kukimoto, J. Cryst. Growth **68**, 27 (1984).
[4] H. Kroemer, J. Vac. Sci. Technol. B **1**, 126 (1983).
[5] H. Mariette, V. Thierry-Mieg, A. Etcheberry, J. C. Guillaume, A. Marbeuf, and M. Rommeluere, J. Cryst. Growth **53**, 413 (1981).
[6] W. Korber and K. W. Benz, J. Cryst. Growth **73**, 179 (1985).
[7] J. S. Yuan, M. T. Tsai, C. H. Chen, R. M. Cohen, and G. B. Stringfellow, J. Appl. Phys. **60**, 1346 (1986).
[8] S. Laouliche, A. Ginudi, A. Le Corre, D. Lecrosnier, C. Vaudry, L. Henry, and C. Guillemot, Appl. Phys. Lett. **55**, 2099 (1989).
[9] C. Gaonach, S. Cassette, M. A. DiForte-Poisson, C. Brylinski, M. Champagne, and A. Tardella, Semicond. Sci. Technol. **5**, 322 (1990).

[10]J. Nishizawa, S. Yoshida, and M. Koike, J. Cryst. Growth **78**, 274 (1986).
[11]T. Kato, T. Matsumoto, and T. Ishida, J. Cryst. Growth **71**, 728 (1985).
[12]J. F. Chen, J. C. Chen, Y. S. Lee, Y. W. Choi, K. Xie, P. L. Liu, W. A. Anderson, and C. R. Wie, J. Appl. Phys. **67**, 3711 (1990).
[13]P. Cova, R. A. Masut, J. F. Currie, A. Bensaada, R. Leonelli, and C. Anh Tran, Can. J. Phys. **69**, 412 (1991).
[14]W. J. Bartels, J. Vac. Sci. Technol. B **1**, 338 (1983).
[15]J. Hornstra and W. J. Bartels, J. Cryst. Growth **44**, 513 (1978).
[16]C. R. Wie, H. M. Kim, and K. M. Lau, SPIE Proc. **877**, 41 (1988).
[17]K. L. Kavanagh, M. A. Capasso, L. W. Hobbs, J. C. Barbour, P. M. J. Marée, W. Schaff, J. W. Mayer, D. Petit, J. M. Woodal, J. A. Stroscio, and R. M. Feenstra, J. Appl. Phys. **64**, 4843 (1988).
[18]M. A. G. Halliwell, Adv. X-Ray Anal. **33**, 61 (1990).
[19]S. F. Fang, K. Adomi, S. Iyer, H. Morkoç, H. Zabel, C. Choi, and N. Otsuka, J. Appl. Phys. **68**, R31 (1990).
[20]K. Kamigaki, H. Sakashita, H. Kato, M. Nakayama, N. Sano, and H. Terauchi, Appl. Phys. Lett. **49**, 1071 (1986).
[21]S. K. Ghandi and J. E. Ayers, Appl. Phys. Lett. **53**, 1204 (1988).
[22]W. Stolz, F. E. G. Guimaraes, and K. Ploog, J. Appl. Phys. **63**, 492 (1988).
[23]V. Swaminathan and A. T. Macrander, *Material Aspects of GaAs and InP Based Structures* (Prentice Hall, Englewood Cliffs, NJ, 1991), p. 191.
[24]H. Asai and K. Oe, J. Appl. Phys. **54**, 2052 (1983).
[25]A. Onton, M. R. Lorenz, and W. Reuter, J. Appl. Phys. **42**, 3420 (1971).
[26]J. W. Matthews and A. E. Blakeslee, J. Cryst. Growth, **27**, 118 (1974).
[27]M. J. McCollum, M. H. Kim, S. S. Bose, B. Lee, and G. E. Stillman, Appl. Phys. Lett. **53**, 1868 (1988).
[28]D. Morris, A. P. Roth, R. A. Masut, C. Lacelle, and J. L. Brebner, J. Appl. Phys. **64**, 4135 (1988).
[29]K. Buckland, H. W. Dinges, and E. Kuphal, J. Appl. Phys. **53**, 655 (1982).
[30]P. Merle, D. Auvergne, and H. Mathieu, Phys. Rev. B **15**, 2032 (1977).
[31]F. H. Pollak and M. Cardona, Phys. Rev. **172**, 816 (1968).
[32]C. P. Kuo, S. K. Vong, R. M. Cohen, and G. B. Stringfellow, J. Appl. Phys. **57**, 5428 (1985).
[33]I. J. Fritz, P. L. Gourley, and L. R. Dawson, Appl. Phys. Lett. **51**, 1004 (1987).